MICROCHIP

# TB3108

## TRIAC Dimmable LED Driver Using PIC12HV752

**WARNING**

**This symbol indicates that building or using the system described in this document will expose you to electric shock.**

**Only persons experienced in electrical manufacture should use this document to complete the system described. FAILURE TO FOLLOW PROPER SAFETY PRECAUTIONS COULD RESULT IN PERMANENT INJURY OR DEATH DUE TO ELECTRIC SHOCK HAZARDS. To avoid risk of injury from electric shock, do not build, or use, the system described in this document without implementing proper safety measures.**

*Microchip Technology Inc. makes no representation that the system shown in this document meets any standards that govern the performance, consumer safety, or electrical interference characteristics of the system described herein. We recommend that you contact the applicable governing body for your geography to determine the standards to which you should manufacture your system.*

*Authors: Kristine Angelica Sumague*
*Mark Pallones*
*Microchip Technology Inc.*

## INTRODUCTION

This technical brief describes a LED driver solution that is compatible with a traditional TRIAC dimmer. Microchip's PIC12HV752 microcontroller manages the whole circuit solution with a minimal firmware code.

The PIC12HV752 is a low-cost 8-pin chip with on-chip core independent peripherals that are suitable for power conversion applications. These peripherals are the Complementary Output waveform Generator (COG) and the Hardware Limit Timer (HLT). Other peripherals include I/O ports, a Fixed Voltage Reference (FVR), Comparators, a Digital-to-Analog Converter (DAC), Timers, a Capture/Compare/PWM (CCP) and an Analog-to-Digital Converter (ADC).

The solution described in this technical brief has the following specifications:

- TRIAC Dimmable
- Active 0.95 Power Factor Correction (PFC)
- 90-240 VAC Input
- 20 VDC/325 mA max. output

## HIGH PF FLYBACK CONVERTER

The design solution which will be discussed in this technical brief uses a high Power Factor (PF) flyback converter operating in Critical Conduction Mode (boundary between continuous and discontinuous Inductor Current mode). This topology is basically a conventional flyback, except that it does not have a bulk capacitor after the full-bridge rectifier. The absence of the bulk capacitor allows the rectified sinusoid to be used as input of the converter rather than a fixed DC voltage.

What makes this topology an attractive solution for a TRIAC Dimmable application is its inherent Power Factor Correction (PFC). The incandescent lamp works well with a TRIAC dimmer because it is purely resistive. Therefore, in order to design a LED driver compatible with TRIAC dimmer, the input characteristics of the LED driver should be resistive, too. PFC can make the LED driver look like a pure resistor from the AC input side by making the input line current in-phase with the input line voltage.

Aside from the high PF, there are other advantages this topology can offer. The advantages can be summarized as follows:

- Isolation between the AC mains and the converter output (this is desirable for safety requirements)
- Minimizes the needs of heat sinks. Critical Conduction Mode (CrCM) ensures low switching losses of the MOSFET
- High PF reduces dissipation in the bridge rectifier

- Low part count helps reduce cost and meets small form factor
- A small size cheaper film capacitor replaces the bulky and costly high-voltage electrolytic capacitor after the full-bridge rectifier

## THEORY OF OPERATION

Figure 1 shows the simplified circuit of a TRIAC Dimmable High PF Flyback LED Driver. The PIC12HV752 microcontroller controls the circuit at the primary side, using on-chip core independent peripherals. The COG peripheral provides a Pulse-Width Modulated (PWM) signal which drives the input of the MCP1416 MOSFET driver to turn-on/turn-off the MOSFET (Q1). The rising edge of the PWM is controlled by the HLT or the C1 comparator, while the falling edge is controlled by the C2 comparator. The input of C1 is derived from the voltage of the auxiliary winding of transformer T1, which is compared with VSS to detect the zero crossing of the auxiliary winding voltage (VAUX). The input of C2 is voltage across the $R_{SENSE}$ resistor, which is compared to the DAC output. The DAC output depends on its $V_{REF}$, which is connected to the input wave shape signal, derived from the rectified input signal through a simple voltage divider.

**FIGURE 1: TRIAC DIMMABLE LED DRIVER SIMPLIFIED SCHEMATIC**

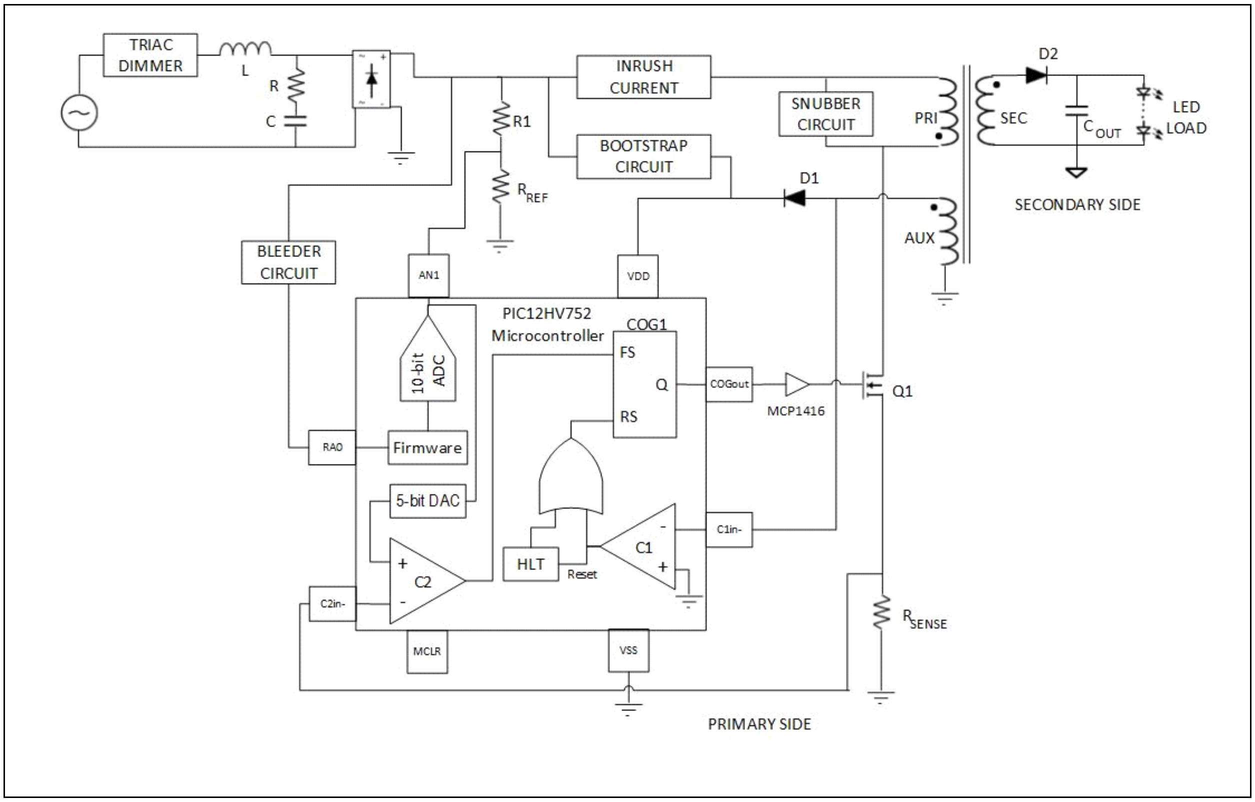


The key advantage of the primary side control is the implementation of the PFC function, which is achieved through the feed forward method along with Peak Current mode control.

The details of circuit operation from start-up to steady state condition will be discussed in the next sections. To simplify the discussion, the following assumptions will be made:

- The line voltage is perfectly sinusoidal
- All components are ideal
- Zero-current detection delay is negligible

### Start-up Operation

When applying the AC input voltage, the base voltage of transistor Q4 in the bootstrap circuit shown in Figure 2 is increasing. When there is enough base voltage, Q4 turns on and diode (D14) is forward biased. The voltage across the base of Q4 is held up to 10V by Zener diode D13. When Q4 turns on, the collector current flows through $R_C$ and D14 to increase the VDD of the PIC12HV752. When VDD is high enough (usually the minimum VDD of the microcontroller) HLT, COG, DAC, ADC and comparators are initialized. After initialization, the HLT emits a pulse at 58 kHz to turn on Q1 initially. This will energize the primary inductance of T1 and transfer the magnetizing current to produce

 

$V_{AUX}$ when Q1 turns off. Once the rectified $V_{AUX}$ has reached 10 Volts, the forward voltage of D14 drops below 0.7 Volts. This allows D14 not to conduct and Q4 to turn off. Once Q4 is off, $V_{DD}$ is supplied by $V_{AUX}$. It is important that Q4 always be off during normal circuit operation to avoid power dissipation on Q4. Q4 remains off as long as there is enough $V_{AUX}$. The operation of the bootstrap circuit is depicted through the waveform shown in Figure 3.

**FIGURE 2: BOOTSTRAP CIRCUIT**

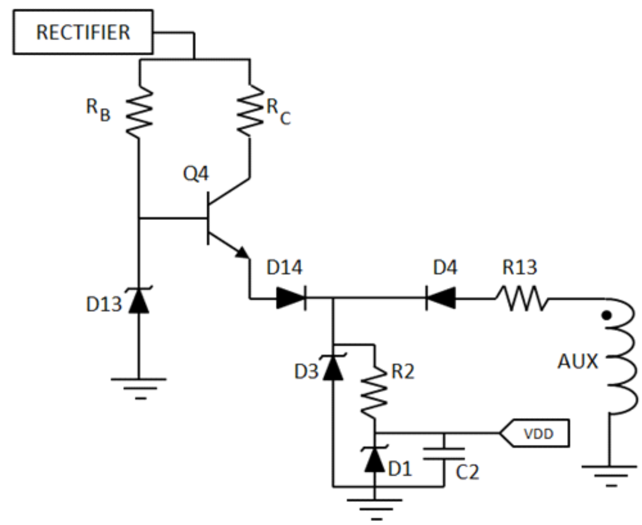


**FIGURE 3: BOOTSTRAP WAVEFORM**

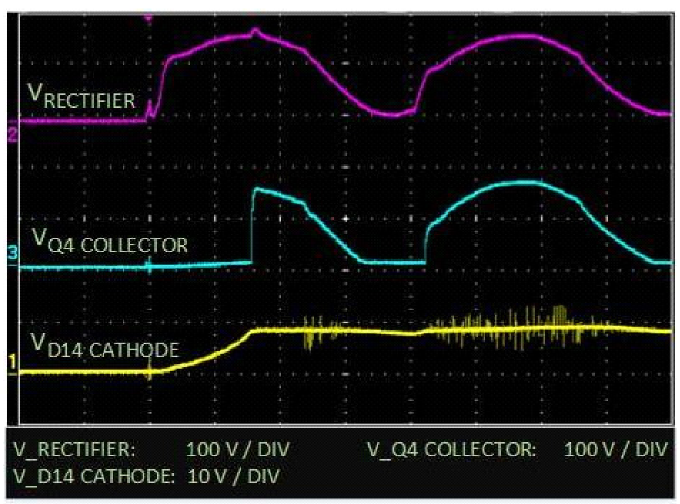


 

### Steady State Operation

When Q1 is on, the secondary diode (D2) is off and the voltage across the T1 primary magnetizing inductance ($V_{LP}$) is equal to $V_{IN}$ (*t*) (see Equation 1). $V_{IN}$ (*t*) is the rectified input voltage which is equal to peak input voltage ($V_{PK}$) multiplied by the rectified input line phase angle $2\pi f_L t$ ($f_L = 1/T_L$; $f_L$ is the line voltage frequency and $T_L$ is the line voltage period). To simplify the notation, let $2\pi f_L t$ be equal to θ (see Equation 2).

**EQUATION 1: PRIMARY MAGNETIZING INDUCTANCE VOLTAGE**

$$V_{LP} = V_{IN}(t)$$

**EQUATION 2: INPUT VOLTAGE**

$$V_{IN}(t) = V_{PK} * |\sin\theta|$$

Additionally, when Q1 is on the primary inductance current ($I_{LP}$) is increasing linearly. This current will flow through the $R_{SENSE}$ resistor. The voltage drop across $R_{SENSE}$ is used as a sense voltage ($V_{SENSE}$) to translate $I_{LP}$ (see Equation 3).

**EQUATION 3: VOLTAGE ACROSS RSENSE**

$$V_{SENSE} = R_{SENSE} * I_{LP}$$

Due to the turn-on event of Q1, $I_{LP}$ is usually affected by a noise which is eventually reflected to $V_{SENSE}$ (see Figure 4). In order to prevent this switching noise from causing a false trigger, the COG peripheral uses the comparator blanking timers to count off a few cycles.

**FIGURE 4: SWITCHING NOISE ON VSENSE**

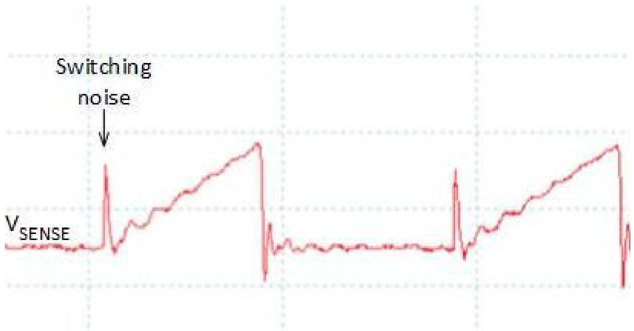


$V_{SENSE}$ is compared with the DAC voltage ($V_{DAC}$) (this is also the peak current set point) by the C2 comparator. $V_{DAC}$ is derived from the rectified input voltage through a voltage divider so that it follows the rectified input and forces the peak current of primary inductance ($I_{LPK}$) to be synchronized and proportional to the rectified input. This is how the circuit achieves the PFC function. Equation 4 represents the $V_{DAC}$ voltage.

**EQUATION 4: DAC VOLTAGE**

$$V_{DAC} = V_{PK} * |\sin\theta| \left(\frac{R_{REF}}{R1 + R_{REF}}\right)\left(\frac{DAC<0:4>}{2^5}\right)$$

When $V_{SENSE}$ reaches $V_{DAC}$, Q1 turns off and HLT is reset. The duration while Q1 is on ($T_{ON}$) can be derived using Equation 1. $V_{LP}$ in Equation 1 is equal to the primary inductance ($L_P$) multiplied by the rate of change of $I_{LP}$ with respect to time. Equation 5 shows this relationship.

**EQUATION 5: PRIMARY MAGNETIZING INDUCTANCE VOLTAGE**

$$V_{PK} * |\sin\theta| = L_P \frac{dI_{LP}}{dt}$$

Deriving the primary inductance current with respect to $V_{PK}$ leads to Equation 6.

**EQUATION 6: PRIMARY INDUCTANCE CURRENT**

$$I_{LP} = \int_0^{T_{ON}} \frac{V_{PK}\,|\sin\theta|}{L_P}\,dt = \frac{V_{PK}\,|\sin\theta|\,T_{ON}}{L_P}$$

$I_{LP}$ is also equal to $I_{PK}$ sin θ since the $I_{PK}$ is enveloped by the rectified sinusoid. Using this relationship and Equation 6 we can solve $T_{ON}$ (see Equation 7).

### EQUATION 7: Q1 TURN-ON TIME

$$T_{ON} = \frac{L_P\, I_{PK}\, |\sin\theta|}{V_{PK}\, |\sin\theta|} = \frac{L_P\, I_{PK}}{V_{PK}}$$

It can be observed in Equation 7 that $T_{ON}$ is not affected by the θ phase angle. Therefore, $T_{ON}$ is constant over the instantaneous line cycle. However, $T_{ON}$ tends not to become constant at minimum voltage on both sides of the rectified sinusoid. This is due to a slight input offset caused by Peak Current mode control comparator C2.

When Q1 is off, D2 is on and the voltage output ($V_O$) is equal to the voltage of T1 secondary inductance winding ($V_{LS}$). The primary magnetizing current is transferred to the secondary winding as secondary inductance current ($I_{LS}$). The $I_{LS}$ decreases linearly and the duration time before it reaches zero is defined by $T_{OFF}$ (see Equation 8 to Equation 10 in deriving $T_{OFF}$).

Using Equation 8, $I_{LS}$ current can be derived as shown in Equation 9.

### EQUATION 8: VOLTAGE OUTPUT

$$V_O = V_{LS} = L_S\, \frac{dI_{LS}}{dt}$$

### EQUATION 9: SECONDARY MAGNETIZING CURRENT

$$I_{LS} = \int_0^{T_{OFF}} \frac{V_O\, dt}{L_S} = \frac{V_O T_{OFF}}{L_S}$$

$I_{LS}$ is also equal to n $I_{PK}$ sin θ and $L_S$ is equal to $L_P/n^2$ where n is T1's primary to secondary winding turns ratio $N_P/N_S$. Substituting to Equation 9 and solving for $T_{OFF}$ yields to Equation 10 below.

### EQUATION 10: Q1 TURN-OFF TIME

$$T_{OFF} = \frac{\frac{L_P}{n^2}\, n\, I_{PK}\, |\sin\theta|}{V_O} = \frac{L_P\, I_{PK}\, |\sin\theta|}{n\, V_O}$$

In Equation 10, $T_{OFF}$ is a function of θ, therefore, it is variable over the instantaneous line cycle.

As stated earlier, the design is working in CrCM. In order to ensure this conduction mode operation, Q1 should turn on again when $I_{LS}$ reaches zero. This is made possible through zero current detection (ZCD) using C1. C1 detects $I_{LS}$ zero crossing based on $V_{AUX}$.

Figure 5 shows a timing diagram to visualize the control operation from start-up to steady state.

### FIGURE 5: LED DRIVER CONTROL TIMING DIAGRAM

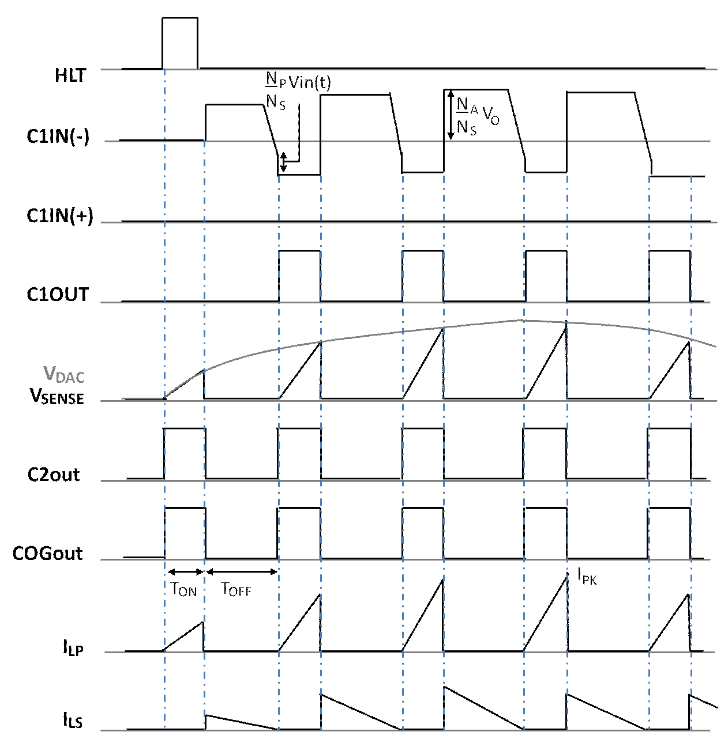

Since the circuit works at CrCM the sum of Equation 7 and Equation 10 is equal to the switching period $T_S$ (see Equation 11).

#### EQUATION 11: Q1 SWITCHING PERIOD

$$T_s = T_{ON} + T_{OFF} = \frac{L_P\, I_{PK}}{V_{PK}}\left[1 + \frac{V_{PK}|\sin\theta|}{n\,V_O}\right]$$

The switching frequency $F_S$ is the inverse of $T_S$ shown in Equation 12.

#### EQUATION 12: Q1 SWITCHING FREQUENCY

$$F_S = \frac{V_{PK}}{L_P\, I_{PK}} \cdot \frac{1}{1+\frac{V_{PK}|\sin\theta|}{n\,V_O}}$$

In Equation 12, it is observable that $F_S$ varies with the instantaneous line voltage since it is a function of θ. The switching Duty Cycle (D) is the ratio between $T_{ON}$ and $T_S$, and varies with instantaneous voltage as well (see Equation 13).

#### EQUATION 13: DUTY CYCLE

$$D = \frac{T_{ON}}{T_S} = \frac{1}{1+\frac{V_{PK}|\sin\theta|}{n\,V_O}}$$

### Power Transfer

The average input current ($I_{P\ AVG}$) can be obtained by averaging the area under $I_{LP}$ (see Equation 14). This current is sinusoidal and in-phase with $V_{IN}(t)$. As a result, the LED driver behaves much like a resistor and exhibits a PF close to unity (see Figure 6).

#### EQUATION 14: AVERAGE INPUT CURRENT

$$I_{P\ AVG} = \frac{1}{2}\, I_{PK}|\sin\theta|\, D = \frac{1}{2}\, \frac{V_{PK}|\sin\theta| D^2 T_S}{L_P}$$

#### FIGURE 6: VIN(t) AND $I_{PK}$ WAVEFORM

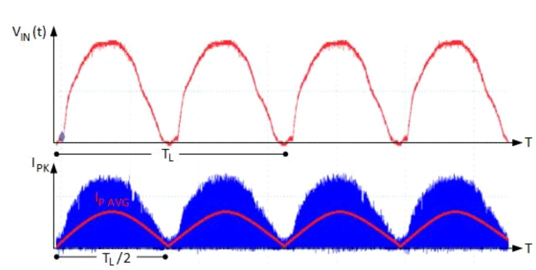


The input power, $P_{IN\ AVG}$, drawn by the LED driver is derived by averaging the product of $V_{IN}$ (t) and $I_{P\ AVG}$ over one half line cycle $T_L$. (see Equation 15).

#### EQUATION 15: AVERAGE INPUT POWER

$$P_{IN\ AVG} = \int_0^{TL/2} V_{IN}(t)\ I_{P\ AVG}\ dt = \frac{1}{4}\,\frac{V_{PK}{}^2 D^2\, T_S}{L_P}$$

$P_{IN\ AVG}$ can be a function of $V_{IN\ RMS}$ (see Equation 16).

#### EQUATION 16: AVERAGE INPUT POWER WITH RESPECT TO INPUT RMS VOLTAGE

$$P_{IN\ AVG} = \frac{V_{IN\ RMS}{}^2}{\left(\frac{2\,L_P}{D^2\,T_S}\right)} = \frac{V_{IN\ RMS}{}^2}{R_{EFFECTIVE}}\ ; R_{EFFECTIVE} = \frac{2\,L_P}{D^2\,T_S}$$

In Equation 16, $R_{EFFECTIVE}$ is the input equivalent resistance of the LED driver seen by the AC main input.

In order to relate the $P_{IN\ AVG}$ to LED average current $I_{LED}$, the relationship of output power $P_O$ with input power $P_{IN}$ of LED driver will be used. This relationship is defined on Equation 17.

#### EQUATION 17: OUTPUT POWER

$$P_{O} = \eta\, P_{IN}$$

In Equation 17, $P_O$ is equal to the product of $V_O$ and $I_{LED}$ where $V_O$ is also equal to the LED string forward voltage. $P_{IN}$ is equal to $P_{IN\ AVG}$ and η is the efficiency of the LED driver. Deriving the equation for $I_{LED}$ from this relationship leads to Equation 18.

#### EQUATION 18: LED CURRENT

$$I_{LED} = \eta\, \frac{V_{INRMS}{}^2}{V_O\, R_{EFFECTIVE}}$$

In Equation 18, $I_{LED}$ is function of $V_{IN\ RMS}$. This is the same RMS voltage that the TRIAC dimmer alters when dimming the LED. Therefore, through the relationship between $I_{LED}$ and $V_{RMS}$ shown in Equation 18, LED brightness can be controlled by the TRIAC dimmer.

## ADDITIONAL CIRCUIT

In Figure 1, there are some circuit blocks included in the design in order to improve the reliability.

### Inrush Current Circuit

The Inrush current circuit is an active circuit that protects the primary side components by suppressing the large input current spikes. These large current spikes are induced in the input line when the TRIAC in the dimmer is fired. A large spike will also create an input current oscillation that may cause the TRIAC to misfire.

### Bleeder Circuit

The bleeder circuit draws additional current in order to maintain the TRIAC holding current at low input line voltage. Not maintaining the required holding current of the TRIAC will cause the TRIAC to misfire. The circuit is composed of the bleeder resistor and a bipolar transistor, which is turned on by the microcontroller only when certain rectified low input voltage is detected through the ADC. This is an efficient way to implement a bleeder since it will not consume additional power when it is not needed. Figure 7 shows the switching timing of the bleeder circuit.

**FIGURE 7: SWITCHING OF BLEEDER CIRCUIT**

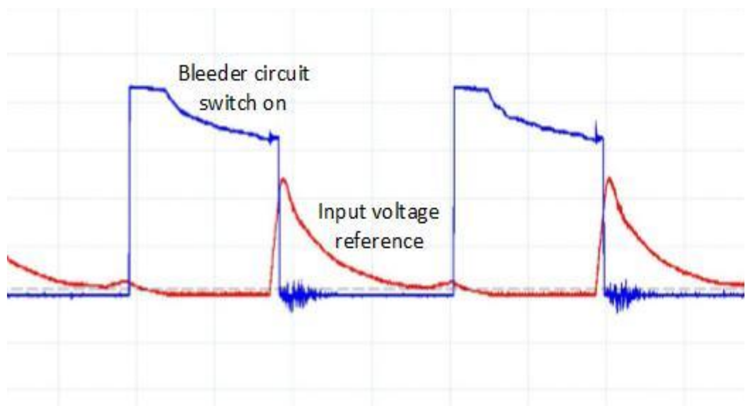


### Snubber Circuit

The snubber circuit is used to protect Q1 from a large voltage spike caused by the leakage inductance of T1. When Q1 turns off, the energy from the leakage inductance is reflected back to primary winding. The snubber circuit dissipates this energy to minimize the voltage spike. The circuit consists of a fast switching diode in series with a parallel combination of a capacitor and resistor. In some designs, an additional Zener transil clamp is included to minimize the power loss at light load.

## ACTUAL CIRCUIT

The actual circuit of the TRIAC Dimmable LED Driver is provided in **Appendix B: "LED Driver Schematic"**. The value of components shown are to be treated only as a starting point. They need to be tuned for each design. The design must be verified and optimized across the entire range of operating conditions.

## FIRMWARE

The circuit design of the LED driver seems complex as it appears but the firmware is straightforward (see Figure 8). It appears that the firmware's overhead is small and mainly consists of initializing the core independent peripherals. The pins on the PIC® device are configured according to their function. After the pins have been configured, the peripherals are setup and turned on. During the initialization, the internal connections and functions of the peripherals are established. The ADC detects the status of the TRIAC dimmer. If the rectified input voltage sampled by the ADC exceeds the TRIAC minimum holding current threshold voltage, the bleeder circuit turns off, otherwise, it will turn on. Before the bleeder circuit turns on, a certain delay is required to evaluate the state of TRIAC dimmer.

**FIGURE 8: FIRMWARE FLOW**

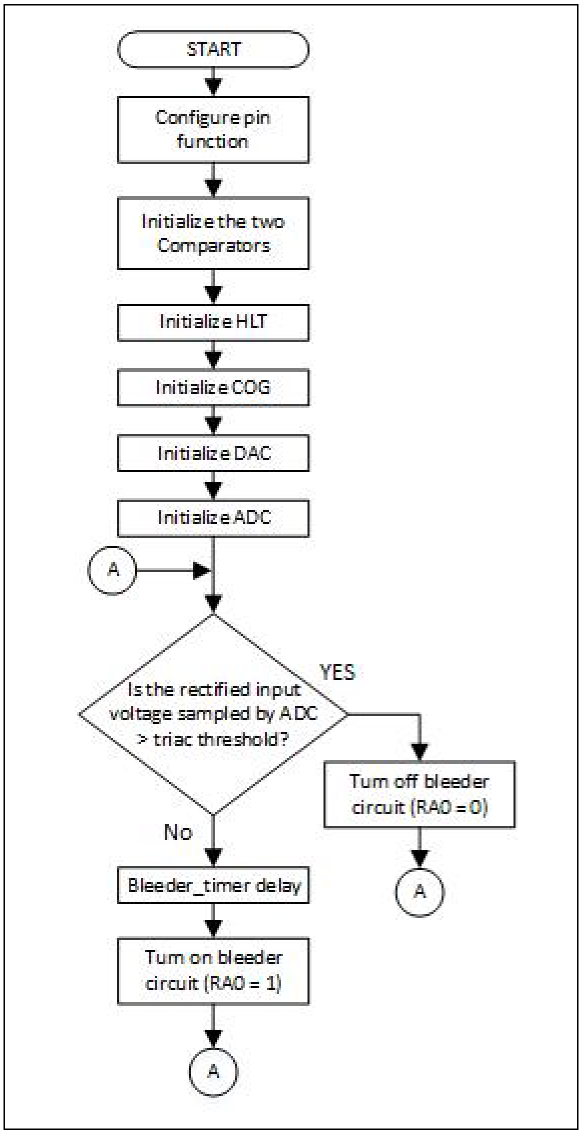


## MCU PERIPHERAL CONFIGURATION

Figure 9 and Table 1 summarize the MCU peripheral configuration.

**FIGURE 9: PERIPHERAL CONFIGURATION**

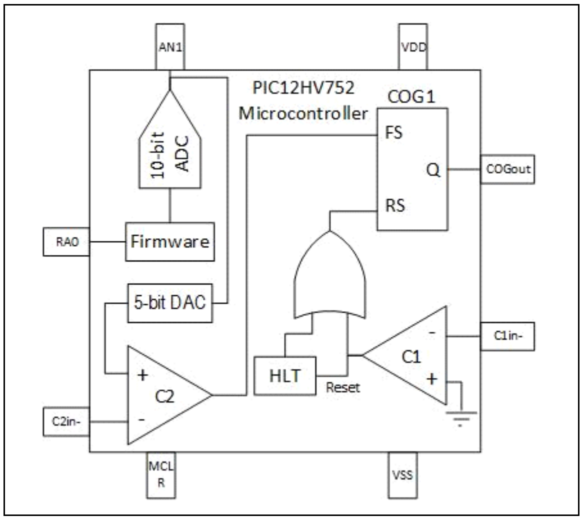


**TABLE 1: PIC12HV752 PIN CONNECTION**

| Pin No. | Name | Function | Circuit Connection |
|---|---|---|---|
| 1 | VDD | Supply Voltage | Bootstrap |
| 2 | C2IN- | Comparator 2 negative input | Sensing resistor |
| 3 | C1IN- | Comparator 1 negative input | Auxiliary regulated voltage |
| 4 | $\overline{MCLR}$ | Memory Clear | ICSP™ (In-Circuit Serial Programmer™) |
| 5 | COGOUT0 | Complementary Output Generator | MOSFET Driver |
| 6 | AN1/VREF | Analog-to-Digital | Rectifier input voltage through voltage divider |
| 7 | I/O | Output | Bleeder circuit |
| 8 | VSS | Ground connection | Ground |

## COG (Complementary Output Generator)

The main purpose of the Complementary Output Generator (COG) in the circuit design is to convert two separate input events into a single PWM output. The COG uses two independently selectable event sources to generate the PWM. These event sources are the rising event, RS, and the falling event, FS, set by the two comparators and the HLT. The event input detection may be selected as level detection or edge-triggered. The rising source and falling source operate as edge-triggered and level sensitive, respectively.

COG output Q is set to high only when a rising edge triggers the rising source input. During this time, the COG turns on the MOSFET. The MOSFET turns off when a low-voltage level is detected on the falling source of the COG. Figure 10 describes the operation of the COG.

### FIGURE 10: COG OPERATION

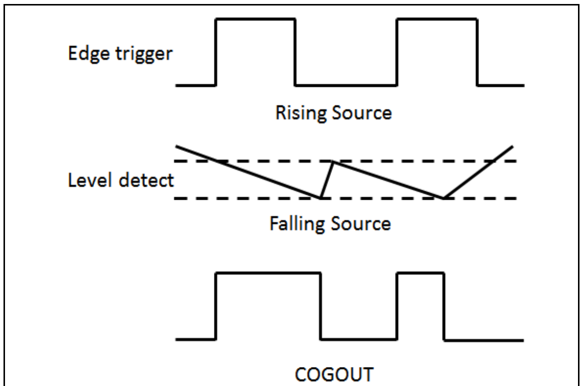


During MOSFET switching, noise may occur that could result in false triggering. This can be avoided by using a blanking scheme. Blanking disregards the event inputs for a short period of time. Since the oscillator of the PIC12HV752 runs at 8 MHz and the blanking count register is set to 4, the resulting blanking time would range from 500 ns to 625 ns on both falling and rising sources. Equation 19 describes the blanking calculation.

### EQUATION 19: COG BLANKING RANGE

$$T_{min} = \frac{Count}{F_{COG\_Clock}}\ ;\ T_{max} = \frac{Count+1}{F_{COG\_Clock}}$$

Where:

$$Count = \begin{cases} GxBLKR < 3:0 > = 4, & rising\ event \\ GxBLKF < 3:0 >= 4, & falling\ event \end{cases}$$

$$F_{COG\_clock} = 8\ MHz$$

## HLT (Hardware Limit Timer)

The primary purpose of the HLT is to act as a timed hardware limit to be used in conjunction with asynchronous analog feedback applications. The external Reset source synchronizes the HLT timer with the analog application.

When the external Reset source occurs before the HLT timer and HLT period match, the HLT timer resets for the next period and prevents its output from going active. However, if the external Reset source fails to generate a signal within the expected time, allowing the HLT timer and HLT period to match, then the HLT output becomes active.

The HLT is configured to be internally connected to the rising source of the COG. HLT provides a rising edge to the COG to initiate the start-up of the converter. The HLT time is set through the equation as shown below in Equation 20:

### EQUATION 20: HLT TIME

$$HLT\ Time = (HLTPR1 + 2)\left(\frac{4}{F_{osc}}\right)$$

Where: $HLTPR1 = 32$

$$F_{osc} = 8\ MHz$$

## COMPARATORS

Comparators are used to interface analog circuits to a digital circuit by comparing two analog voltages and providing a digital indication of their relative magnitudes. The comparator outputs can be applied to the COG module and can be configured as a closed-loop analog feedback to the COG, thereby creating a PWM controlled in an analog way.

The output of C1 is ORed to the HLT and acts as the rising source of the COG, while the output of C2 is the falling source of the COG. These two comparators act as zero-cross detection and peak current detection on the circuit, respectively. The output of C1 continually resets HLT during the operation of the converter.

## DAC (Digital-to-Analog Converter)

A 5-bit DAC module is used to translate the rectified input voltage. It is internally connected to the positive input of C2. It operates in Full-Range mode with the DAC output voltage as shown in Equation 21 where $V_{SRC}$ is the voltage across the voltage divider network (see Figure 1).

**EQUATION 21: DAC VOLTAGE**

$$V_{DAC} = \left((V_{SRC} +)\left(\frac{DACR<4:0>}{2^5}\right)\right)$$

$$\text{Where: } DACR < 4:0 > = \begin{cases} 1, & at\ 230V \\ 7, & at\ 115V \end{cases}$$

### ADC (Analog-to-Digital Converter)

The ADC converts the input signal into a 10-bit binary representation. This value is calculated using the ADC equation shown in Equation 22.

The ADC samples and translates the rectified input voltage in order to control the toggling of pin 7 (RA0). RA0 becomes low when the voltage sampled by the ADC is greater than the minimum voltage required to maintain the holding current of the TRIAC dimmer, otherwise, RA0 will be high.

**EQUATION 22: ADC VOLTAGE**

$$V_{ADC} = \frac{V_{SRC}(2^{10} - 1)}{V_{ADC\ REF}}$$

## PERFORMANCE

Table 2 and Table 3 show the measured dimming performance of the LED driver operating at 230V and 115V, respectively. Its graphical representation is shown in Figure 11 wherein the dimming is controlled by the TRIAC output voltage.

**TABLE 2: MEASURED DIMMING PERFORMANCE AT 230V INPUT VOLTAGE**

| 230 $V_{IN}$ | |
|---|---|
| **TRIAC Output Voltage ($V_{RMS}$)** | **LED Current (mA)** |
| 230.1 | 297.33 |
| 218.5 | 262.21 |
| 172 | 162.63 |
| 160.1 | 141.03 |
| 149.1 | 122.81 |
| 139.4 | 104.57 |
| 130.1 | 85.16 |
| 119 | 72.24 |
| 109.8 | 62.9 |
| 101 | 53.11 |
| 90.1 | 41.95 |

**TABLE 2: MEASURED DIMMING PERFORMANCE AT 230V INPUT VOLTAGE**

| 230 $V_{IN}$ | |
|---|---|
| **TRIAC Output Voltage ($V_{RMS}$)** | **LED Current (mA)** |
| 80.3 | 32.24 |
| 68.2 | 22.81 |
| 60.2 | 17.86 |
| 50.15 | 12.11 |

**TABLE 3: MEASURED DIMMING PERFORMANCE AT 115V INPUT VOLTAGE**

| 115 $V_{IN}$ | |
|---|---|
| **TRIAC Output Voltage ($V_{RMS}$)** | **LED Current (mA)** |
| 115.5 | 300.39 |
| 100.5 | 225.22 |
| 90.8 | 186.03 |
| 80.5 | 148.73 |
| 70.7 | 115.49 |
| 60.7 | 85.23 |
| 50.23 | 61.65 |
| 41.2 | 41.19 |
| 29.99 | 18.84 |

**FIGURE 11: DIMMING PERFORMANCE**

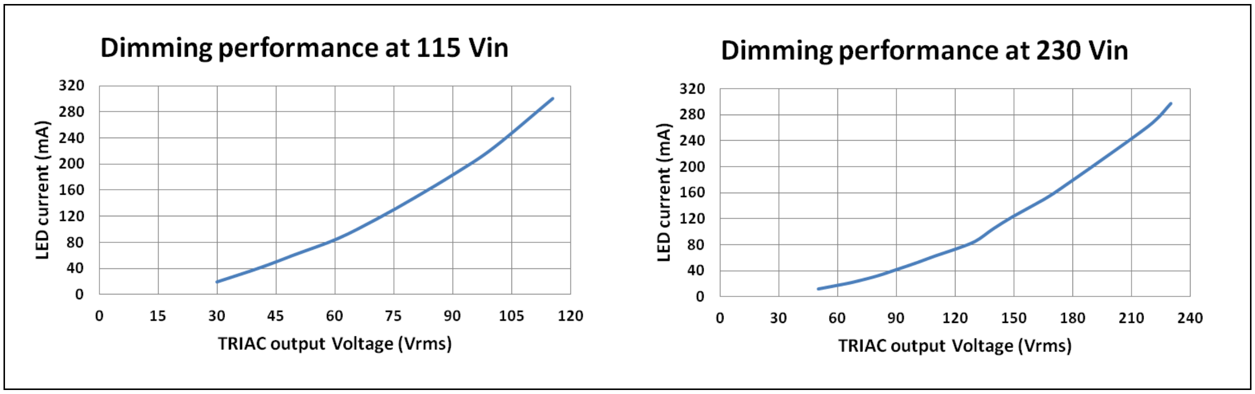


## POSSIBLE DESIGN IMPROVEMENTS

Even a high Power Factor device like the LED driver discussed in this technical brief represents a capacitive load. This is because of the filter implemented at the input side of the circuit. This LC filter can produce a high voltage ringing derived from input current oscillation when the TRIAC in the dimmer initially fires. The voltage ringing makes the TRIAC current drop below the holding current and switch off and on again several times during the cycles, resulting in severe flickering and a humming sound.

**FIGURE 12: FLICKERING WAVEFORM**

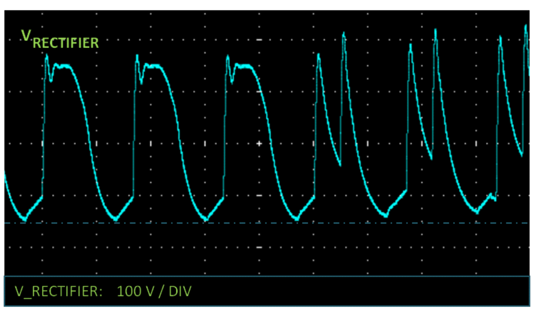


During the first three cycles in the rectified line voltage shown in Figure 12, the TRIAC has recovered after firing and continues the conduction. However, after the three cycles, the rectified input waveform changed showing that the TRIAC is turning on and off. This input line event produces flickering and a humming sound.

For a smooth dimming and a quiet operation, the challenge is to avoid unwanted TRIAC switching, caused by the ringing that occurs when the TRIAC is initially fired. The input filter of the LED driver design presented in this technical brief requires an optimization to avoid this problem and ensures that the line waveform will not be altered.

## CONCLUSION

This technical brief describes a PIC microcontroller-based solution controlling the LED driver that is compatible with traditional TRIAC dimmers. With the PIC12HV752, the analog control mainly runs by itself and only requires small firmware overhead. This enables users to add algorithms in order to improve design performance, bring intelligence to the system, or measure any parameter.

## APPENDIX A: LED DRIVER EQUATION DERIVATION

### EXAMPLE A-1: $I_{P\ AVG}$ DERIVATION

$$V = \frac{Ldi}{dt}$$

$$di = \frac{Vdt}{L}$$

$$I_{PK} = \frac{V_{IN}(t)}{L_P} DT_S$$

Where: $V_{IN}(t) = V_{PK}\sin(2\pi f_L t)$

Let $f_L = \frac{1}{T_L}$

$$V_{IN}(t) = V_{PK}\sin\left(\frac{2\pi t}{T_L}\right)$$

Substitute $V_{IN}(t)$ to $I_{PK}$ equation

$$I_{PK} = \frac{V_{PK}\sin\left(\frac{2\pi t}{T_L}\right)}{L_P} DT_S$$

To get the average input current, the equation below must be evaluated

$$I_{P\ AVG} = \frac{1}{T_S}\int_0^{T_S}\frac{1}{2}I_{PK}dt$$

$$I_{P\ AVG} = \frac{1}{T_S}\ x\ \frac{1}{2}\ x\ I_{PK}\int_0^{T_S}\ dt$$

Integrating and Substituting $I_{PK}$ to the equation

$$I_{P\ AVG} = \frac{1}{T_S}\ x\ \frac{1}{2}\ x\ \frac{V_{IN}(t)}{L_P}DT_S\left[\int_0^{DT_S}dt - \int_{DT_S}^{T_S}0dt\right]$$

$$I_{P\ AVG} = \frac{1}{T_S}x\ \frac{1}{2}x\ \frac{V_{IN}(t)}{L_P}DT_S\ x\ DT_S$$

Simplifying the equation results to:

$$I_{P\ AVG} = \frac{V_{IN}(t)}{2L_P}D^2T_S$$

**EXAMPLE A-2: $P_{IN\ AVG}$ DERIVATION (CONTINUED)**

$$P_{IN\ AVG} = \frac{2}{T_L}\int_0^{\frac{T_L}{2}} V_{IN}(t)I_{IN}(t)dt$$

$$P_{IN\ AVG} = \frac{2}{T_L}\int_0^{\frac{T_L}{2}} \frac{V_{PK}{}^2 sin^2\left(\frac{2\pi t}{T_L}\right)D^2T_S}{2L_P}dt$$

$$P_{IN\ AVG} = \frac{2}{T_L}\frac{V_{PK}{}^2D^2T_S}{2L_P}\int_0^{\frac{T_L}{2}} sin^2\left(\frac{2\pi t}{T_L}\right)dt$$

Solve for the integral equation: $\int_0^{\frac{T_L}{2}} sin^2\left(\frac{2\pi t}{T_L}\right)dt$

$$\int_0^{\frac{T_L}{2}} sin^2\left(\frac{2\pi t}{T_L}\right)dt = \int_0^{\frac{T_L}{2}} \frac{1-\cos 2\left(\frac{2\pi t}{T_L}\right)}{2}dt$$

$$\int_0^{\frac{T_L}{2}} sin^2\left(\frac{2\pi t}{T_L}\right)dt = \int_0^{\frac{T_L}{2}} \frac{1}{2}dt - \int_0^{\frac{T_L}{2}} \frac{\cos 2\left(\frac{2\pi t}{T_L}\right)}{2}dt$$

$$\int_0^{\frac{T_L}{2}} sin^2\left(\frac{2\pi t}{T_L}\right)dt = \frac{1}{2}t\,\Big|_0^{\frac{T_L}{2}} - \frac{1}{2}\int_0^{\frac{T_L}{2}} \cos 2\left(\frac{2\pi t}{T_L}\right)dt$$

Simplify the integral equation $\int_0^{\frac{T_L}{2}} \frac{\cos 2\left(\frac{2\pi t}{T_L}\right)}{2}dt$ by letting:

$$u = 2\left(\frac{2\pi t}{T_L}\right) = \frac{4\pi t}{T_L}$$

Derivative of $u$ results to:

$$du = \frac{4\pi}{T_L}dt$$

Simplified equation for $\int_0^{\frac{T_L}{2}} \frac{\cos 2\left(\frac{2\pi t}{T_L}\right)}{2}dt$ is:

$$\int_0^{\frac{T_L}{2}} \frac{\cos 2\left(\frac{2\pi t}{T_L}\right)}{2}dt = \frac{1}{2}\int_0^{\frac{T_L}{2}} \cos u\ du$$

$$\frac{1}{2}\int_0^{\frac{T_L}{2}} \cos u\ du = \frac{1}{2}\sin u + c$$

$$\frac{1}{2}\int_0^{\frac{T_L}{2}} \frac{\cos 2\left(\frac{2\pi t}{T_L}\right)}{2}dt = \frac{1}{2}sin\frac{4\pi t}{T_L}\Big|_0^{\frac{T_L}{2}}$$

Substitute to the resulted value to $\int_0^{\frac{T_L}{2}} sin^2\left(\frac{2\pi t}{T_L}\right)dt$ :

$$\int_0^{\frac{T_L}{2}} sin^2\left(\frac{2\pi t}{T_L}\right)dt = \frac{1}{2}t\,\Big|_0^{\frac{T_L}{2}} - \frac{1}{2}sin\frac{4\pi t}{T_L}\Big|_0^{\frac{T_L}{2}}$$

$$\int_0^{\frac{T_L}{2}} sin^2\left(\frac{2\pi t}{T_L}\right)dt = \frac{1}{2}\left(\frac{T_L}{2} - 0\right) - \frac{1}{2}\left(sin\frac{4\pi\left(\frac{T_L}{2}\right)}{T_L} - sin0\right)$$

**EXAMPLE A-3: $P_{IN\ AVG}$ DERIVATION (CONTINUED)**

$$\int_0^{\frac{T_L}{2}} sin^2\left(\frac{2\pi t}{T_L}\right) dt = \frac{T_L}{4}$$

Substitute to $P_{IN\ AVG}$ equation:

$$P_{IN\ AVG} = \frac{2}{T_L}\frac{{V_{PK}}^2 D^2 T_S}{2L_P}\int_0^{\frac{T_L}{2}} sin^2\left(\frac{2\pi t}{T_L}\right) dt$$

$$P_{IN\ AVG} = \frac{2}{T_L}\frac{{V_{PK}}^2 D^2 T_S}{2L_P}\left(\frac{T_L}{4}\right)$$

$P_{IN\ AVG}$ results to:

$$P_{IN\ AVG} = \frac{{V_{PK}}^2 D^2 T_S}{4L_P}$$

 

## APPENDIX B: LED DRIVER SCHEMATIC

### FIGURE B-1: TRIAC DIMMABLE LED DRIVER SCHEMATIC

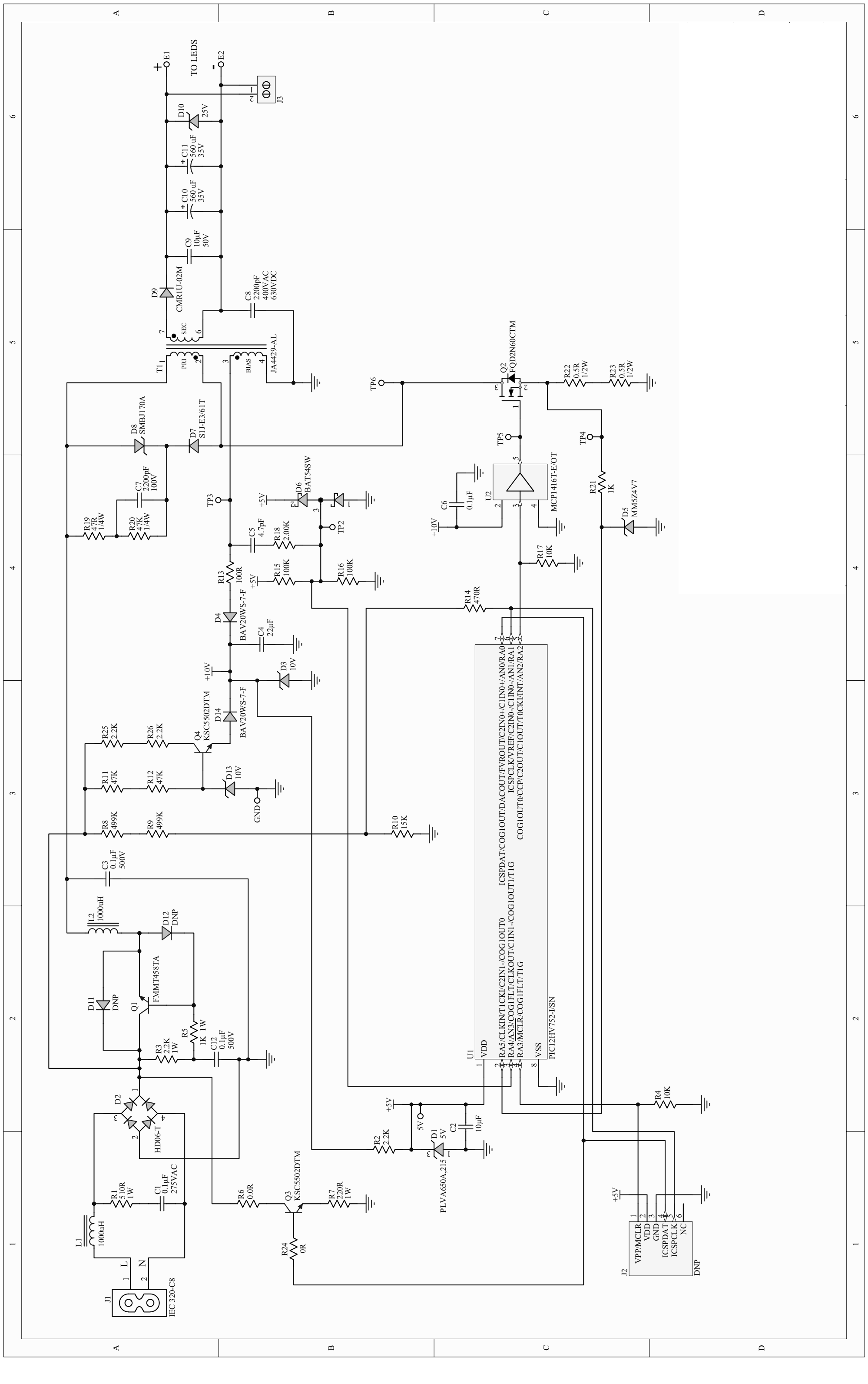

**Note the following details of the code protection feature on Microchip devices:**

- Microchip products meet the specification contained in their particular Microchip Data Sheet.
- Microchip believes that its family of products is one of the most secure families of its kind on the market today, when used in the intended manner and under normal conditions.
- There are dishonest and possibly illegal methods used to breach the code protection feature. All of these methods, to our knowledge, require using the Microchip products in a manner outside the operating specifications contained in Microchip's Data Sheets. Most likely, the person doing so is engaged in theft of intellectual property.
- Microchip is willing to work with the customer who is concerned about the integrity of their code.
- Neither Microchip nor any other semiconductor manufacturer can guarantee the security of their code. Code protection does not mean that we are guaranteeing the product as “unbreakable.”

Code protection is constantly evolving. We at Microchip are committed to continuously improving the code protection features of our products. Attempts to break Microchip's code protection feature may be a violation of the Digital Millennium Copyright Act. If such acts allow unauthorized access to your software or other copyrighted work, you may have a right to sue for relief under that Act.



**QUALITY MANAGEMENT SYSTEM CERTIFIED BY DNV**

**ISO/TS 16949**

**Trademarks**



Printed on recycled paper.

ISBN: 978-1-63276-315-0

*Microchip received ISO/TS-16949:2009 certification for its worldwide headquarters, design and wafer fabrication facilities in Chandler and Tempe, Arizona; Gresham, Oregon and design centers in California and India. The Company's quality system processes and procedures are for its PIC® MCUs and dsPIC® DSCs, KEELOQ® code hopping devices, Serial EEPROMs, microperipherals, nonvolatile memory and analog products. In addition, Microchip's quality system for the design and manufacture of development systems is ISO 9001:2000 certified.*

# Worldwide Sales and Service

## AMERICAS

**Corporate Office**
2355 West Chandler Blvd.
Chandler, AZ 85224-6199
Tel: 480-792-7200
Fax: 480-792-7277
Technical Support:
http://www.microchip.com/support
Web Address:
www.microchip.com

**Atlanta**
Duluth, GA
Tel: 678-957-9614
Fax: 678-957-1455

**Austin, TX**
Tel: 512-257-3370

**Boston**
Westborough, MA
Tel: 774-760-0087
Fax: 774-760-0088

**Chicago**
Itasca, IL
Tel: 630-285-0071
Fax: 630-285-0075

**Cleveland**
Independence, OH
Tel: 216-447-0464
Fax: 216-447-0643

**Dallas**
Addison, TX
Tel: 972-818-7423
Fax: 972-818-2924

**Detroit**
Novi, MI
Tel: 248-848-4000

**Houston, TX**
Tel: 281-894-5983

**Indianapolis**
Noblesville, IN
Tel: 317-773-8323
Fax: 317-773-5453

**Los Angeles**
Mission Viejo, CA
Tel: 949-462-9523
Fax: 949-462-9608

**New York, NY**
Tel: 631-435-6000

**San Jose, CA**
Tel: 408-735-9110

**Canada - Toronto**
Tel: 905-673-0699
Fax: 905-673-6509

## ASIA/PACIFIC

**Asia Pacific Office**
Suites 3707-14, 37th Floor
Tower 6, The Gateway
Harbour City, Kowloon
Hong Kong
Tel: 852-2943-5100
Fax: 852-2401-3431

**Australia - Sydney**
Tel: 61-2-9868-6733
Fax: 61-2-9868-6755

**China - Beijing**
Tel: 86-10-8569-7000
Fax: 86-10-8528-2104

**China - Chengdu**
Tel: 86-28-8665-5511
Fax: 86-28-8665-7889

**China - Chongqing**
Tel: 86-23-8980-9588
Fax: 86-23-8980-9500

**China - Hangzhou**
Tel: 86-571-8792-8115
Fax: 86-571-8792-8116

**China - Hong Kong SAR**
Tel: 852-2943-5100
Fax: 852-2401-3431

**China - Nanjing**
Tel: 86-25-8473-2460
Fax: 86-25-8473-2470

**China - Qingdao**
Tel: 86-532-8502-7355
Fax: 86-532-8502-7205

**China - Shanghai**
Tel: 86-21-5407-5533
Fax: 86-21-5407-5066

**China - Shenyang**
Tel: 86-24-2334-2829
Fax: 86-24-2334-2393

**China - Shenzhen**
Tel: 86-755-8864-2200
Fax: 86-755-8203-1760

**China - Wuhan**
Tel: 86-27-5980-5300
Fax: 86-27-5980-5118

**China - Xian**
Tel: 86-29-8833-7252
Fax: 86-29-8833-7256

**China - Xiamen**
Tel: 86-592-2388138
Fax: 86-592-2388130

**China - Zhuhai**
Tel: 86-756-3210040
Fax: 86-756-3210049

## ASIA/PACIFIC

**India - Bangalore**
Tel: 91-80-3090-4444
Fax: 91-80-3090-4123

**India - New Delhi**
Tel: 91-11-4160-8631
Fax: 91-11-4160-8632

**India - Pune**
Tel: 91-20-3019-1500

**Japan - Osaka**
Tel: 81-6-6152-7160
Fax: 81-6-6152-9310

**Japan - Tokyo**
Tel: 81-3-6880- 3770
Fax: 81-3-6880-3771

**Korea - Daegu**
Tel: 82-53-744-4301
Fax: 82-53-744-4302

**Korea - Seoul**
Tel: 82-2-554-7200
Fax: 82-2-558-5932 or
82-2-558-5934

**Malaysia - Kuala Lumpur**
Tel: 60-3-6201-9857
Fax: 60-3-6201-9859

**Malaysia - Penang**
Tel: 60-4-227-8870
Fax: 60-4-227-4068

**Philippines - Manila**
Tel: 63-2-634-9065
Fax: 63-2-634-9069

**Singapore**
Tel: 65-6334-8870
Fax: 65-6334-8850

**Taiwan - Hsin Chu**
Tel: 886-3-5778-366
Fax: 886-3-5770-955

**Taiwan - Kaohsiung**
Tel: 886-7-213-7830

**Taiwan - Taipei**
Tel: 886-2-2508-8600
Fax: 886-2-2508-0102

**Thailand - Bangkok**
Tel: 66-2-694-1351
Fax: 66-2-694-1350

## EUROPE

**Austria - Wels**
Tel: 43-7242-2244-39
Fax: 43-7242-2244-393

**Denmark - Copenhagen**
Tel: 45-4450-2828
Fax: 45-4485-2829

**France - Paris**
Tel: 33-1-69-53-63-20
Fax: 33-1-69-30-90-79

**Germany - Dusseldorf**
Tel: 49-2129-3766400

**Germany - Munich**
Tel: 49-89-627-144-0
Fax: 49-89-627-144-44

**Germany - Pforzheim**
Tel: 49-7231-424750

**Italy - Milan**
Tel: 39-0331-742611
Fax: 39-0331-466781

**Italy - Venice**
Tel: 39-049-7625286

**Netherlands - Drunen**
Tel: 31-416-690399
Fax: 31-416-690340

**Poland - Warsaw**
Tel: 48-22-3325737

**Spain - Madrid**
Tel: 34-91-708-08-90
Fax: 34-91-708-08-91

**Sweden - Stockholm**
Tel: 46-8-5090-4654

**UK - Wokingham**
Tel: 44-118-921-5800
Fax: 44-118-921-5820

03/25/14